Regulation of DNA damage and immune response pathways by post-translational protein modification

Dijk, M.

5

How dextran sulfate affects C1-inhibitor activity: a model for polysaccharide potentiation

Madelon Dijk, Jolande Holkers, Patrick Voskamp, Bruno M. Giannetti, Willem-Jan Waterreus, Harrie A. van Veen and Navraj S. Pannu

Published as:
How dextran sulfate affects C1-inhibitor activity: a model for polysaccharide potentiation Structure 24, 2182-2189 (2016)

Abstract

C1-inhibitor is a key inhibitor of the complement and contact activation systems, and mutations in the protein can cause hereditary angioedema. Through an unknown mechanism, polysaccharides can increase C1-inhibitor activity against some of its target proteases. Here we present the crystal structures of the serine protease inhibitor (serpin) domain of active C1-inhibitor by itself and in complex with dextran sulfate. Unlike previously described interactions of serpins with polysaccharides, the structures and isothermal titration calorimetry experiments together reveal that dextran sulfate binds to C1-inhibitor's F1 helix with low affinity and does not invoke an allosteric change. Furthermore, one dextran sulfate molecule can bind multiple C1-inhibitor molecules. We propose that in a C1-inhibitor-protease-polysaccharide ternary complex, negatively charged polysaccharides link C1-inhibitor's positively charged F1 helix to positively charged autolysis loops of proteases. The described mechanism elegantly explains previous experiments, showing that polysaccharide potentiation is increased against proteases with a greater positive charge in the autolysis loop.

Introduction

C1-inhibitor replacement therapy is an established treatment for hereditary angioedema – a disease characterized by recurrent episodes of swelling of the skin or mucosa as a result of an acute, localized increase in vascular permeability[1]. Additionally, C1-inhibitor therapy has been studied in sepsis, ischemia-reperfusion injury, and autoimmune diseases such as neuromyelitis optica[2,3,4].

C1-inhibitor is a plasma glycoprotein that belongs to the superfamily of serine protease inhibitors (serpins)[5]. Serpins are suicide inhibitors and in the active form, the reactive center loop protrudes from the bulk of the protein and presents the P1-P1' residues as a substrate for proteolytic attack. Upon binding of the target protease, the reactive center loop inserts into the serpin's central β-sheet while the attached protease moves to the opposite pole of the serpin, causing the disruption of the protease's active site[6]. Comparably, insertion of the reactive center loop into the central β-sheet can cause the spontaneous transition from a metastable active form to a more stable latent conformation.

C1-inhibitor is the only known plasma protein inhibitor of classical complement pathway serine proteases C1s and C1r. Furthermore, it inactivates MASP-1 and MASP-2 proteases from the mannose-binding lectin pathway, plasmin and tissue plasminogen activator from the fibrinolytic system, factor XIIa and plasma kallikrein from the contact activation system, and the coagulation system proteases factor XIa and thrombin[1]. Given its wide range of biological activities, a potent therapy optimization would involve the fine-tuning and enhancement of C1-inhibitor activity against a particular protease[7].

As observed for other serpins, glycosaminoglycans (GAGs) and negatively charged polysaccharides such as dextran sulfate have been shown to affect C1-inhibitor activity. For example, significant potentiation of C1-inhibitor by heparin against C1s was demonstrated by various techniques[8-10]. It was also shown that oversulfated chondroitin sulfate – a heparin contaminant that has been linked to severe clinical adverse events – potentiates C1-inhibitor activity on the complement pathway[11]. Interestingly in view of therapy refinement, C1-inhibitor potentiation by GAGs has appeared to be different toward the various target proteases[8].

The atomic mechanism behind the effect of polyanions on C1-inhibitor remains to be elucidated. Heparin binds to antithrombin and heparin cofactor II at helix D and causes an allosteric change in these serpins[12,13]. Unraveling the mechanism behind the enhancement of C1-inhibitor activity by polysaccharides may contribute to the development of molecules that improve C1-inhibitor's efficiency and specificity.

Here we present the crystal structures of the serpin domain of C1-inhibitor in its active form by itself and in complex with dextran sulfate. These structures and our isothermal titration calorimetry studies show that dextran sulfate binds to multiple C1-inhibitor molecules with low affinity at C1-inhibitor's F1 helix and does not invoke an allosteric change.

Results and discussion

To elucidate how polysaccharides interact with C1-inhibitor we purified the recombinant protein, lacking the first 96 residues of C1-inhibitor's heavily glycosylated N-terminus, from the milk of transgenic rabbits. The remaining serpin domain of C1-inhibitor has previously been shown to have full inhibitory activity[14]. Subsequently, C1-inhibitor was crystallized by itself, as well as co-crystallized with dextran sulfate. Crystals of recombinant human C1-inhibitor diffracted to 2.1 Å, whereas crystals of the protein in complex with dextran sulfate diffracted to 2.9 Å (Table 1).

Table 1: Data collection and refinement statistics

	C1-inhibitor	C1-inhibitor with dextran sulfate
Data collection		
Space group	$P\,2_12_12_1$	C2
Cell dimensions		
a, b, c (Å)	57.40, 75.48, 203.89	112.10, 197.42, 56.78
α, β, γ (°)	90.00, 90.00, 90.00	90.00, 103.31, 90.00
Resolution (Å)	2.1	2.9
Wilson plot B-factor	32.9	77.7
R_{pim}	0.057 (0.570)*	0.089 (1.987)*
CC(1/2)	0.998 (0.790)	0.996 (0.117)
<I/σI>	13.9 (1.6)	7.2 (0.4)
Completeness (%)	99.93	98.68
Multiplicity	4.7	3.0
Refinement		
No. of unique reflections	43663	24919
Molecules in ASU	2	2
R_{work}/ R_{free}	0.197/0.257	0.239/0.281
RMSD		
Bond lengths (Å)	0.025	0.011
Bond angles (°)	2.19	1.57

* Numbers in brackets are values for the highest resolution shell. For the uncomplexed structure, the highest resolution shell is 2.10 to 2.16 Å. For the complex structure, the highest resolution shell is 2.90 to 3.08 Å.

Structure of active C1-inhibitor

We first solved the overall structure of uncomplexed C1-inhibitor (Fig. 1a). The full exposure of the relatively short reactive center loop (shown in red and pink) characterizes inhibitory serpins in their active form. Clear electron density is seen for the reactive center loop residues Arg444 to Val448 (shown in red). These residues stack with the same reactive center loop residues but in the opposite direction to the other C1-inhibitor molecule present in the asymmetric unit. Both C1-inhibitor molecules lack electron density for reactive center loop residues Ala443 to Ser441 (shown in pink). Residues Arg444 and Thr445 within the reactive

center loop are the substrate P1 and P1' residues that are responsible for trapping the target protease. In the latent and cleaved conformation of C1-inhibitor, the reactive center loop inserts between strand s3A and s5A of the central β-sheet, rendering the inhibitor inactive.

The model contains two disulfide bridges at Cys101-Cys406 and Cys108-Cys183 that stabilize the structure.

Lys307, previously predicted to be involved in GAG binding, specifically stabilizes the reactive center loop in its active conformation by hydrogen bonding to the carboxyl group of Ala436[15]. Notably, an A436T mutation causes type II hereditary angioedema and results in a non-cleavable reactive center loop[16]. Our structure shows that the threonine residue likely increases the interaction with Lys307 or Lys306 to prevent cleavage, leading to insertion of the exposed reactive center loop into strand A of another C1-inhibitor molecule. Importantly, these results also explain why heparin interacts more strongly with the latent form of C1-inhibitor, as in its active conformation the reactive center loop hinders exposure of the positive charge of Lys306 and Lys307[15].

Comparing the latent and active C1-inhibitor structures not only shows the expected shifts in β-sheet A required for loop insertion, but also displays a conformational change in strand s3C and s4C, a region that is expected to shift during latent transition as well[17]. The strands follow the C-terminal end of the reactive center loop as it is inserted into the β-sheet A and are shifted down and outward in the latent C1-inhibitor molecule.

Structure of active C1-inhibitor bound to dextran sulfate

We next analyzed the crystal structure of C1-inhibitor co-crystallized with dextran sulfate. The crystallographic asymmetric unit again contains two C1-inhibitor molecules with their reactive center loops fully exposed and in close proximity to each other (displayed as a ribbon and electrostatic representation in two different orientations in Fig. 1b; a single C1-inhibitor molecule is shown in Fig. 1c). The negatively charged dextran sulfate neutralizes the positive charge around the F1 helix of the C1-inhibitor molecules. Supporting our model, mutating the F1 helix residue Lys284 has been shown to affect the binding of C1-inhibitor to glycosaminoglycans[18]. Arg287 is another nearby residue that was predicted to be important for glycosaminoglycan binding, but its positive charge is stabilized by hydrogen bonding to the amino group of Lys284 of the other C1-inhibitor molecule[18].

The overall structures of C1-inhibitor by itself and in complex with dextran sulfate are very similar: the root mean square deviation is 0.486 Å for C-α positions of all residues apart from Ala437-Phe449 of the reactive center loop. Thus, in contrast to what has been described for other serpins, binding of dextran sulfate does not invoke an allosteric change. The similarity of the structures is consistent with the results obtained by circular dichroism showing no allosteric change upon polysaccharide binding[10]. A saccharide electrostatically interacts with Lys284 of one C1-inhibitor molecule and Lys299 of the other C1-inhibitor molecule at the edge of the protein (Fig. 1d, showing the $2F_o - F_c$ electron density for the modelled dextran sulfate saccharides). This novel interaction is the first time a charge neutralization mechanism with low affinity binding has been observed for a serpin and a polysaccharide.

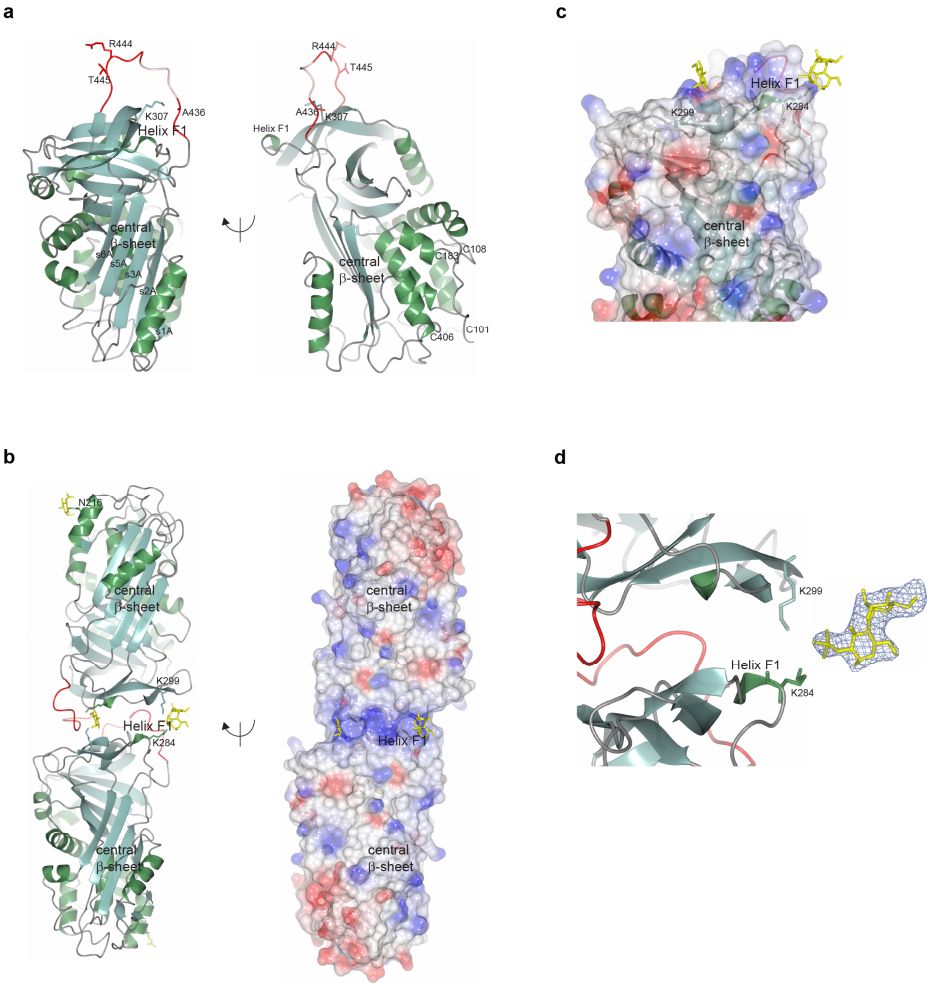

Figure 1. Structure of active C1-inhibitor by itself and bound to dextran sulfate
(a) The overall structure of active C1-inhibitor in two different orientations. The fully exposed reactive center loop is shown in red where the loop has clear electron density and light pink where the loop is disordered. The P1 Arg444 residue and P1′ Thr445 residue are displayed, along with residue Lys307 that stabilizes the reactive center loop by hydrogen bonding to the carboxyl oxygen of Ala436. Helix F1 is the polyanion binding site. The central β-sheet A and the disulfide bridges at Cys101-Cys406 and Cys108-Cys183 are also labeled. (b) The overall structure of active C1-inhibitor bound to dextran sulfate in two different orientations, showing a ribbon diagram and an electrostatic surface of C1-inhibitor with positively charged regions in blue and negatively charged regions in red. C1-inhibitor is positively charged at the dextran sulfate (in yellow) binding site. Three dextran sulfate saccharides were built in the crystal structure and link Lys284 from helix F1 of one C1-inhibitor molecule to Lys299 on the other C1-inhibitor molecule. The glycosylation at Asn216 was also modeled in the complex crystal structure. (c) Electrostatic surface of the top of one C1-inhibitor molecule with dextran sulfate (in yellow). The reactive center loop is shown in red. The side chains for Lys284 and Lys299 (the residues interacting with the saccharide molecules) are also shown. (d) 2Fo−Fc electron density map (blue mesh) of a disaccharide of dextran sulfate contoured at 1.1σ. All figures were produced by ccp4mg[23].

The modelled polysaccharide molecules are in a large channel between symmetry-related C1-inhibitor molecules: the channel has sufficient space for a dextran sulfate molecule of 5 kDa. However, only 3 saccharide molecules could be modelled while the density of the other polysaccharides is too weak for modelling, probably due to the random linkage and sulfation pattern of dextran sulfate. The monosaccharide molecules interacting with Lys284 to Lys299 from the same C1-inhibitor molecule are about 20 Å apart.
Importantly, although negatively charged polysaccharides can enhance C1-inhibitor activity against proteases, its inhibiting activity could be impeded if the polysaccharide would induce C1-inhibitor multimerization over protease binding.

Stoichiometry and binding affinity of dextran sulfate binding to C1-inhibitor
To assess the binding of dextran sulfate to C1-inhibitor, we performed isothermal titration calorimetry (ITC) experiments, for which 5, 10 or 20 kDa dextran sulfate was added to full-length C1-inhibitor (Fig. 2a-c). Supporting our crystal structure, the ITC results show 1 low-affinity binding site on C1-inhibitor for the polysaccharide independent of its size. Multiple C1-inhibitor molecules can bind to 1 molecule of dextran sulfate: the stoichiometry of the C1-inhibitor-dextran sulfate complex is 1:1 for 5 kDa, 2:1 for 10 kDa and 3:1 for 20 kDa dextran sulfate. Based on the model curves from the ITC data, representing the best fit obtained for the data (Fig. 2a-c), we calculated the stoichiometries and binding constants for complex formation in this experimental set-up (Table 2). The low-affinity electrostatic binding is in agreement with previously determined values by several groups[9,10,19].

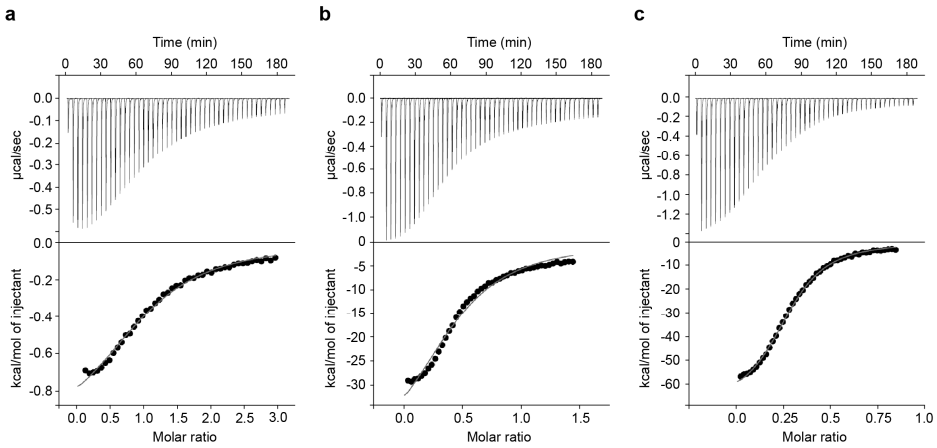

Figure 2. Stoichiometry and binding affinity of dextran sulfate binding to C1-inhibitor
Isothermal titration calorimetry experiments showing the titration of dextran sulfate of different sizes to C1-inhibitor in the sample cell. (a) Titration of 5 kDa dextran sulfate. (b) Titration of 10 kDa dextran sulfate. (c) Titration of 20 kDa dextran sulfate.

Table 2: Binding constants and stoichiometry for the binding of C1-inhibitor to dextran sulfate

Dextran sulfate (kDa)	Binding constant (x10^5 M^{-1})	Stoichiometry
5	1.16±0.12	1.16±0.03
10	1.80±0.21	0.479±0.021
20	8.34±0.28	0.294±0.002

C1s-C1-inhibitor and kallikrein-C1-inhibitor Michaelis complex models

GAG binding to C1-inhibitor can greatly enhance its activity against C1s, while the effect on kallikrein inactivation is minimal. We created models of the Michaelis complex of C1s-C1-inhibitor by superimposing the protease and C1-inhibitor on several previously solved Michaelis serpin-protease complexes, available in the Protein Data Bank (PDB) as 1k9o[20], 1jmo[13], 1oph[21], and 4dy7[22]. Despite the different relative orientation between the serpin and the protease in the different Michaelis complexes published, all of the resulting complexes show C1-inhibitor's helix F1 residues Lys284 and/or Arg287 neighboring autolysis loop residues Lys560 and Arg561. The Michaelis complexes based on PDB entries 1k9o, 1oph, and 4dy7 show C1-inhibitor residue Lys284 in close proximity to C1s residue Lys560 and C1-inhibitor residue Arg287 near C1s residue Arg561 (Fig. 3a, created with 1k9o). Docking the C1-inhibitor and C1s structures using PDB entry 1jmo shows C1-inhibitor residues Arg287 and Lys299 in the close vicinity of C1s residues Lys560 and Arg561, respectively (Fig. 3b). The crystal structure of C1-inhibitor-dextran sulfate revealed that residue Lys299 interacts with saccharide molecules. Notably, both models indicate that a negatively charged polysaccharide molecule would neutralize the repulsive forces between indicated basic side chains, thereby enhancing C1-inhibitor activity. Interestingly, a model for the Michaelis complex of kallikrein and C1-inhibitor based on the Michaelis complex from PDB entry 1k9o (Fig. 3c), shows again that residues Lys284 and Arg287 of C1-inhibitor are in close proximity to the autolysis loop residues Lys147 and Glu150. However, in contrast to C1s, an attractive electrostatic force already exists between C1-inhibitor residue Arg287 and residue Glu150 of kallikrein, so a polyanion would not further promote activity by neutralizing charges. Unlike in the case of C1s described above, all created kallikrein-C1-inhibitor models display a similar interaction between the indicated residues of C1-inhibitor and kallikrein.

Taking together the structures of C1-inhibitor, the proteases C1s and kallikrein, and the Michaelis serpin-protease complexes, negatively charged polysaccharides likely increase the activity of C1-inhibitor by neutralizing at least the positive charges of C1-inhibitor residues in or near the F1 helix, namely Lys284 and Arg287, and possibly C1-inhibitor residue Lys299 and positive residues of the autolysis loop of target proteases. In this mechanism, the saccharide is not in between the protease and inhibitor and thus does not form a 'sandwich' as previously predicted, but instead binds on the outer edge of both the protease and the inhibitor[15]. The positive patches near Lys306 are sterically hindered by the relatively short reactive center loop from forming charge neutralization interactions. Our model provides important insight into how C1-inhibitor activity toward its different targets is sensitive to

potentiation by GAG binding to different extents, depending on the nature of the protease's autolysis loop.

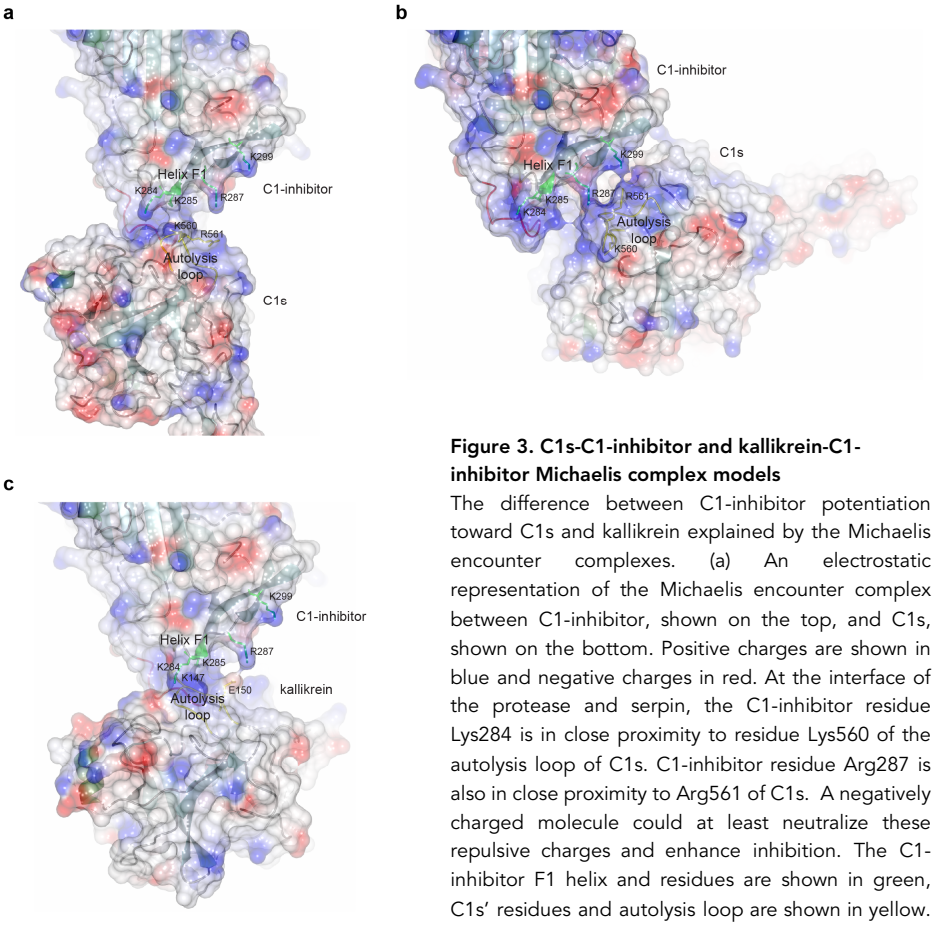

Figure 3. C1s-C1-inhibitor and kallikrein-C1-inhibitor Michaelis complex models

The difference between C1-inhibitor potentiation toward C1s and kallikrein explained by the Michaelis encounter complexes. (a) An electrostatic representation of the Michaelis encounter complex between C1-inhibitor, shown on the top, and C1s, shown on the bottom. Positive charges are shown in blue and negative charges in red. At the interface of the protease and serpin, the C1-inhibitor residue Lys284 is in close proximity to residue Lys560 of the autolysis loop of C1s. C1-inhibitor residue Arg287 is also in close proximity to Arg561 of C1s. A negatively charged molecule could at least neutralize these repulsive charges and enhance inhibition. The C1-inhibitor F1 helix and residues are shown in green, C1s' residues and autolysis loop are shown in yellow. This model is based on the serpin-protease complex from PDB entry 1k9o. (b) An electrostatic representation of the Michaelis encounter complex between C1-inhibitor, shown on the top, and C1s, shown on the bottom. Positive charges are shown in blue and negative charges in red. At the interface of the protease and serpin, the C1-inhibitor residue Arg287 is in close proximity to residue Lys560 of the autolysis loop of C1s. C1-inhibitor residue Lys299 is also in close proximity to Arg561 of C1s. A negatively charged molecule could at least neutralize these repulsive charges and enhance inhibition. The C1-inhibitor residues are shown in green, while C1s' residues and autolysis loop are shown in yellow. This model is based on the serpin-protease complex from PDB entry 1jmo. (c) An electrostatic representation of the Michaelis encounter complex between C1-inhibitor, shown on the top, and kallikrein, shown on the bottom. Positive charges are shown in blue and negative charges in red. At the interface of the protease and serpin, the C1-inhibitor residue Lys284 is in close proximity to residue Lys147 of the autolysis loop of kallikrein, but C1-inhibitor residue Arg287 forms an electrostatic interaction with Glu150 of kallikrein. The C1-inhibitor residues are shown in green, while kallikrein's residues and autolysis loop are shown in yellow. This model is based on the serpin-protease complex from PDB entry 1k9o. All figures were produced by ccp4mg[23].

Supplementary information

Methods

Protein expression, purification and crystallization

Production of recombinant human C1-inhibitor secreted in the milk of transgenic rabbits was performed as previously described[14]. Functionally active C1-inhibitor lacking the first 96 residues, present in negligible amounts in purified C1-inhibitor[14], were separated from intact molecules by a sequence of cation exchange chromatography on SP Sepharose High Performance (GE Healthcare) and affinity chromatography on Jacalin Agarose (Vector Labs). Fractions obtained from the Jacalin Agarose column containing C1-inhibitor lacking the first 96 residues were concentrated to about 10 mg/ml in 20 mM sodium citrate pH 7.0 + 0.15 M NaCl and stored at -70 °C until use. Diffraction quality crystals of active C1-inhibitor were obtained after about 7 days in 20% PEG3350 w/v and 200 mM KF with a crystallization drop size of 1 µl and a protein content of 70% w/v using the sitting-drop vapour diffusion method. These conditions were optimized from initial hits found in both JCSG+ and PACT (Qiagen) screens. For co-crystallization, 11 mg/ml of C1-inhibitor was mixed with 5 kDa dextran sulfate (Sigma-Aldrich) in a 1:2 molar ratio and incubated on ice for an hour. Again, crystallization trials were set up with JCSG+ and PACT screens and initial hits were optimized to obtain the final conditions of 0.1 M SPG (pH 9), 25% w/v PEG 1500 0.1 M MgCl hexahydrate, with crystals appearing after 10 days.

Data collection

Crystals were caught with SPINE sample loops and put in cryoprotectant solution (precipitant solution with 10-15% glycerol) and flash-frozen. Data for the native, active C1-inhibitor were collected at beam line BM14 at the European Synchrotron Radiation Facility (Grenoble, France)[24]. 120 images were collected with an oscillation angle of 1.0 degree and exposure time of 20 s per frame at 100 K. For the C1-inhibitor/dextran sulfate complex crystal, 1074 images were collected with a 0.15 degree oscillation angle and an exposure time of 0.037 s per frame at 100 K on beamline ID23-1[25]. The images were processed with *XDS*[26]. Scaling and merging were done with *AIMLESS* (Evans, 2006) from the *CCP4* suite[27]. The complex crystal diffracted anisotropically as clearly shown in the half set correlations, CC(1/2)[28] for different axes: along the k-axis the CC(1/2) was 0.515 at 2.9 Å, but the CC(1/2) was 0.3 at 3.55 Å along the h-axis and 3.14 Å along the l-axis. Data collection statistics are shown in Table 1.

Structure solution and refinement

The structure of uncomplexed C1-inhibitor was solved by molecular replacement using the latent structure of C1-inhibitor (PDB entry 20AY) as a search model[15]. A vast majority of the model was automatically rebuilt using *Arp/Warp*[29] and refined with *Refmac*[30], coupled with manual fitting using *Coot*[31]. For the C1-inhibitor-dextran sulfate complex, the phase problem was solved by molecular replacement using the native C1-inhibitor structure as a search model. Clear difference density was visible for the dextran sulfate as well as glycosylation sites. The saccharides of dextran sulfate were automatically built with *Coot* using the 'Find ligand' function. The carbohydrate configuration and density were validated with the program *Privateer*[32]: the real space correlation coefficient for the three saccharides built were 0.83, 0.78 and 0.75. The model was refined with *Refmac* and further manual fitting was also performed using *Coot*. For the C1-inhibitor-dextran sulfate model, refinement using different resolution cutoffs and data truncated by the anisotropic diffraction data server was attempted, but no major effect on electron density quality or R-factor statistics was observed: the anisotropic scaling in *Refmac* appeared to appropriately weight down the reflections in the weakly diffracting directions. The final R-factor and R_{free} for uncomplexed C1-inhibitor were 0.197 and 0.257 respectively and 0.239 and 0.281 for C1-inhibitor in complex with dextran sulfate. Refinement statistics are shown in Table 1.

Isothermal titration calorimetry

Measurements were performed on a MicroCal VP-ITC instrument (Malvern Instruments). Recombinant full-length C1-inhibitor was used and prepared as previously described and buffer exchanged into dialysis buffer (20 mM NaCitrate, 10 mM NaCl, pH 7.0) using a Slide-A-Lyzer dialysis cassette (Thermo Scientific). Protein

concentrations were determined by the A_{280} as measured by a Nanodrop2000 (Thermo Scientific), using ε = 26880 M^{-1} cm^{-1}. Dextran sulfate with a mean molecular weight of 5 kDa, 10 kDa or 20 kDa and high sulfation levels (16-20% sulfur) (TdB Consultancy) was dissolved into dialysis buffer. Titrations of 0.15-0.35 mM dextran sulfate into the sample cell containing 25 µM C1-inhibitor were performed at 25 °C. Data was analyzed using the MicroCal ITC-Origin analysis software and for the analysis, the first titration has been removed for 10 kDa and 20 kDa dextran sulfate, while the first two titrations have been removed for 5 kDa. The results are shown in Table 2.

Models of the Michaelis complex of C1s:C1-inhibitor and kallikrein:C1-inhibitor

Using the previously determined structures of the Michaelis serpin-protease complex of alaserpin and trypsin[20] (pdb code 1k9o), heparin cofactor II and thrombin[13] (pdb code 1jmo), alpha-1-antitrypsin and trypsin[21] (pdb code 1oph) and protease nexin-1 and thrombin[22] (pdb code 4dy7) as templates, as well as the structure of C1-inhibitor in complex with dextran sulfate presented here and the previously determined structures of C1s[33] and the catalytic domain of human plasma kallikrein[34], models of the C1s-C1-inhibitor and kallikrein-C1-inhibitor Michaelis complexes were created using the SSM superposition function in the program *Coot*. For the protease nexin-1-thrombin structure, two Michaelis complexes were present in the asymmetric unit; our analysis used the complex that would permit proteolytic cleavage.

Protein data bank accession codes

5DU3 (native structure), 5DUQ (complex with dextran sulfate)

References

1. Davis, A.E., III, Lu, F. & Mejia, P. C1 inhibitor, a multi-functional serine protease inhibitor. Thromb. Haemost 104, 886-893 (2010).
2. Caliezi, C. et al. C1-inhibitor in patients with severe sepsis and septic shock: beneficial effect on renal dysfunction. Crit Care Med 30, 1722-1728 (2002).
3. Lu, F., Fernandes, S.M. & Davis, A.E., III. The effect of C1 inhibitor on myocardial ischemia and reperfusion injury. Cardiovasc. Pathol 22, 75-80 (2013).
4. Levy, M. & Mealy, M.A. Purified human C1-esterase inhibitor is safe in acute relapses of neuromyelitis optica. Neurol. Neuroimmunol. Neuroinflamm 1, e5 (2014).
5. Irving, J.A., Pike, R.N., Lesk, A.M. & Whisstock, J.C. Phylogeny of the serpin superfamily: implications of patterns of amino acid conservation for structure and function. Genome Res 10, 1845-64 (2000).
6. Huntington, J.A., Read, R.J. & Carrell, R.W. Structure of a serpin-protease complex shows inhibition by deformation. Nature 407, 923-926 (2000).
7. Karnaukhova, E. C1-Esterase inhibitor: biological activities and therapeutic applications. J Hematol Thromb Dis 1(2013).
8. Wuillemin, W.A. et al. Potentiation of C1 inhibitor by glycosaminoglycans: dextran sulfate species are effective inhibitors of in vitro complement activation in plasma. J. Immunol 159, 1953-1960 (1997).
9. Caldwell, E.E. et al. Heparin binding and augmentation of C1 inhibitor activity. Arch. Biochem. Biophys 361, 215-222 (1999).
10. Rajabi, M., Struble, E., Zhou, Z. & Karnaukhova, E. Potentiation of C1-esterase inhibitor by heparin and interactions with C1s protease as assessed by surface plasmon resonance. Biochim. Biophys. Acta 1820, 56-63 (2012).
11. Zhou, Z.H., Rajabi, M., Chen, T., Karnaukhova, E. & Kozlowski, S. Oversulfated chondroitin sulfate inhibits the complement classical pathway by potentiating C1 inhibitor. PLoS. One 7, e47296 (2012).
12. Jin, L. et al. The anticoagulant activation of antithrombin by heparin. Proc. Natl. Acad. Sci. U. S. A 94, 14683-14688 (1997).
13. Baglin, T.P., Carrell, R.W., Church, F.C., Esmon, C.T. & Huntington, J.A. Crystal structures of native and thrombin-complexed heparin cofactor II reveal a multistep allosteric mechanism. Proc. Natl. Acad. Sci. U. S. A 99, 11079-11084 (2002).

14. van Veen, H.A. et al. Characterization of recombinant human C1 inhibitor secreted in milk of transgenic rabbits. J. Biotechnol 162, 319-326 (2012).
15. Beinrohr, L. et al. C1 inhibitor serpin domain structure reveals the likely mechanism of heparin potentiation and conformational disease. J. Biol. Chem 282, 21100-21109 (2007).
16. Aulak, K.S. et al. A hinge region mutation in C1-inhibitor (Ala436-->Thr) results in nonsubstrate-like behavior and in polymerization of the molecule. J Biol. Chem 268, 18088-18094 (1993).
17. Mottonen, J. et al. Structural basis of latency in plasminogen activator inhibitor-1. Nature 355, 270-3 (1992).
18. Bos, G.A.C. C-inhibitor potentiation by glycosaminoglycans. PhD thesis (University of Amsterdam) (2003).
19. Rossi, V. et al. Functional characterization of the recombinant human C1 inhibitor serpin domain: insights into heparin binding. J. Immunol 184, 4982-4989 (2010).
20. Ye, S. et al. The structure of a Michaelis serpin-protease complex. Nat. Struct. Biol 8, 979-983 (2001).
21. Dementiev, A., Simonovic, M., Volz, K. & Gettins, P.G. Canonical inhibitor-like interactions explain reactivity of alpha1-proteinase inhibitor Pittsburgh and antithrombin with proteinases. J Biol Chem 278, 37881-7 (2003).
22. Li, W. & Huntington, J.A. Crystal structures of protease nexin-1 in complex with heparin and thrombin suggest a 2-step recognition mechanism. Blood 120, 459-67 (2012).
23. Potterton, L. et al. Developments in the CCP4 molecular-graphics project. Acta Crystallogr. D. Biol. Crystallogr 60, 2288-2294 (2004).
24. Grenoble, E. http://www.embl.fr/services/synchrotron_access/bm14/. (2015).
25. Nurizzo, D. et al. The ID23-1 structural biology beamline at the ESRF. J. Synchrotron. Radiat 13, 227-238 (2006).
26. Kabsch, W. XDS. Acta Crystallogr. D. Biol. Crystallogr 66, 125-132 (2010).
27. Winn, M.D. et al. Overview of the CCP4 suite and current developments. Acta Crystallogr. D. Biol. Crystallogr 67, 235-242 (2011).
28. Karplus, P.A. & Diederichs, K. Linking crystallographic model and data quality. Science 336, 1030-1033 (2012).
29. Perrakis, A., Morris, R. & Lamzin, V.S. Automated protein model building combined with iterative structure refinement. Nat. Struct. Biol 6, 458-463 (1999).
30. Murshudov, G.N. et al. REFMAC5 for the refinement of macromolecular crystal structures. Acta Crystallogr. D. Biol. Crystallogr 67, 355-367 (2011).
31. Emsley, P., Lohkamp, B., Scott, W.G. & Cowtan, K. Features and development of Coot. Acta Crystallogr. D. Biol. Crystallogr 66, 486-501 (2010).
32. Agirre, J., Davies, G., Wilson, K. & Cowtan, K. Carbohydrate anomalies in the PDB. Nat. Chem. Biol 11, 303 (2015).
33. Gaboriaud, C., Rossi, V., Bally, I., Arlaud, G.J. & Fontecilla-Camps, J.C. Crystal structure of the catalytic domain of human complement c1s: a serine protease with a handle. EMBO J 19, 1755-1765 (2000).
34. Tang, J. et al. Expression, crystallization, and three-dimensional structure of the catalytic domain of human plasma kallikrein. J Biol Chem 280, 41077-89 (2005).